



Dynamics of Photoinduced Energy Transfer in Fully and Partially Conjugated Polymers Bearing π -Extended Donor and Acceptor Monomers

Youngseo Kim[†], Na Yeon Kwon[†], Su Hong Park, Min Ju Cho, Dong Hoon Choi* and Sungnam Park*

Department of Chemistry, Research Institute for Natural Sciences, Korea University, Seoul, South Korea

OPEN ACCESS

Edited by:

Rene A. Nome,
State University of Campinas, Brazil

Reviewed by:

Wenkai Zhang,
Beijing Normal University, China
Dibyendu Mondal,
Jain University, India

*Correspondence:

Dong Hoon Choi
dhchoi8803@korea.ac.kr
Sungnam Park
spark8@korea.ac.kr

[†]These authors have contributed
equally to this work

Specialty section:

This article was submitted to
Physical Chemistry and Chemical
Physics,
a section of the journal
Frontiers in Chemistry

Received: 12 September 2020

Accepted: 19 October 2020

Published: 05 November 2020

Citation:

Kim Y, Kwon NY, Park SH, Cho MJ,
Choi DH and Park S (2020) Dynamics
of Photoinduced Energy Transfer in
Fully and Partially Conjugated
Polymers Bearing π -Extended Donor
and Acceptor Monomers.
Front. Chem. 8:605403.
doi: 10.3389/fchem.2020.605403

The photophysical properties of donor (**D**)-acceptor (**A**) polymers were studied by designing two types of polymers, (**D**- σ -**A**)_n and (**D**- π -**A**)_n, with non-conjugated alkyl (sp^3) and π -conjugated (sp^2) linkers using π -extended donor and acceptor monomers that exhibit planar A-D-A structures. The non-conjugated alkyl linker provides structural flexibility to the (**D**- σ -**A**)_n polymers, while the π -conjugated linker retains the rigid structure of the (**D**- π -**A**)_n polymers. Photoinduced energy transfer occurs from the large donor to acceptor units in both polymers. However, the photoinduced energy transfer dynamics are found to be dependent on the conformation of the polymers, where the difference is dictated by the types of linkers between the donor and acceptor units. In solution, intramolecular energy transfer is relatively favorable for the (**D**- σ -**A**)_n polymers with flexible linkers that allow the donor and acceptor units to be proximally located in the polymers. On the other hand, intermolecular (or interchain) energy transfer is dominant in the two polymer films because the π -extended donor and acceptor units in polymers are closely packed. The structural flexibility of the linkers between the donor and acceptor repeating units in the polymers affects the efficiency of energy transfer between the donor and acceptor units and the overall photophysical properties of the polymers.

Keywords: π -extended donor monomer, π -extended acceptor monomer, fully conjugated polymer, partially conjugated polymer, photophysical property, time-resolved fluorescence, energy transfer

INTRODUCTION

Photoinduced energy transfer or charge transfer has been extensively studied using dyad- or triad-type small molecules composed of donor and acceptor moieties (Kuss-Petermann et al., 2012; Wiebeler et al., 2017; Wang et al., 2019). Most studies on the photophysical properties of such molecules have been carried out using boron dipyrromethenes or porphyrin as the donor moiety (Duvanel et al., 2013; Villamaina et al., 2013; Badgurjar et al., 2016). In dyad systems, the donor and acceptor moieties are connected by different types of linkers. The photophysical properties of dyad systems are largely influenced by the linkers between the donor and acceptor moieties; that is, π -conjugated (sp^2 -type) and non-conjugated (or aliphatic, sp^3 -type) linkers. In the past, various donor (**D**)- acceptor (**A**)-type dyad systems have been designed and synthesized as electronic

and optoelectronic materials, including organic photovoltaic cells, organic field effect transistors, and organic light-emitting diodes, and their photophysical properties have been studied (Wu and Brand, 1994; Scholes, 2003; Schwartz, 2003; Murphy et al., 2004; Jones and Bradshaw, 2019). Although the focus has been on small-molecule donors and fullerene receptor systems (Jose et al., 2009; Caprasecca and Mennucci, 2014), a few studies have been performed on the photophysical properties of conjugated polymer systems. For example, Feng et al. introduced a single active polymer by binding a small molecule that exhibits acceptor properties as a side chain moiety to the main chain conjugated polymer with donor properties (Feng et al., 2019; Li et al., 2019). They observed new optoelectronic properties in this polymer by enabling energy transfer or electron transfer in the electronically excited state.

Our group reported polymer solar cells with two different copolymers synthesized by connecting conjugated donor- and acceptor-based macromolecular units (Lee et al., 2017). In our previous study, donor- and acceptor-based macromolecular units were connected using sp^3 and sp^2 linkers, respectively, to investigate the performance of polymer solar cells. The performance of polymer solar cells was found to depend on the linkers between donor- and acceptor-based macromolecular units in the polymers. However, photoinduced energy transfer and photoinduced electron transfer in the two polymers were not able to be studied. Specifically, the donor- and acceptor-based macromolecular units were characterized by a large molecular weight distribution, making it difficult to obtain well-defined spectroscopic features in the UV-visible absorption and steady-state emission spectra. Generally, the photoinduced energy transfer and photoinduced electron transfer process in the polymers are important at the molecular level for optoelectronic devices and need to be comprehensively studied. The photoinduced energy transfer and photoinduced electron transfer in the polymers can be reliably studied by using the polymers with donor- and acceptor-based macromolecular units having a uniform molecular weight.

In this study, we designed and synthesized large A-D-A type donor monomers (**B3TP**, **D**) and A-D1-D2-D1-A type acceptor monomers (**B2IC**, **A**), and utilized them to synthesize two different polymers with non-conjugated alkyl linkers, (**D- σ -A**)_n, and π -conjugated linkers, (**D- π -A**)_n. The structural flexibility of (**D- σ -A**)_n and (**D- π -A**)_n is dictated by the linkers. Overall, (**D- σ -A**)_n is the partially conjugated polymer in which the π -extended donor and acceptor monomers are connected through flexible non-conjugated sp^3 linkers. In contrast, (**D- π -A**)_n is the fully conjugated polymer in which the large donor and acceptor monomers are connected *via* conjugated sp^2 linkers. It is very noteworthy that such polymer structures contain highly π -extended donor and acceptor monomers with a uniform molecular weight, and the large donor and acceptor monomers are alternatively arranged in the polymers. The photophysical properties of (**D- σ -A**)_n and (**D- π -A**)_n in toluene and films were investigated using UV-visible absorption, steady-state emission, and time-resolved fluorescence (TRF) spectroscopy, in conjunction with quantum chemical calculations. The photophysical properties of (**D- σ -A**)_n and (**D- π -A**)_n depend on

the type of linker between the large donor and acceptor units in the polymers. The energy profiles of (**D- σ -A**)_n and (**D- π -A**)_n were found to be similar, but the photoinduced energy transfer from the donor to acceptor units occurred via different pathways. Photoinduced energy transfer in (**D- σ -A**)_n and (**D- π -A**)_n in toluene is mainly due to the intramolecular energy transfer, whereas photoinduced energy transfer in the (**D- σ -A**)_n and (**D- π -A**)_n films proceeds via both intramolecular and intermolecular (or interchain) energy transfer. This is the first report on the photophysical properties of partially and fully conjugated polymers containing well-defined π -extended donor and acceptor monomers. And our current results are expected to be applied to optoelectronic devices using π -conjugated donor-acceptor type polymers.

EXPERIMENTAL

Synthesis

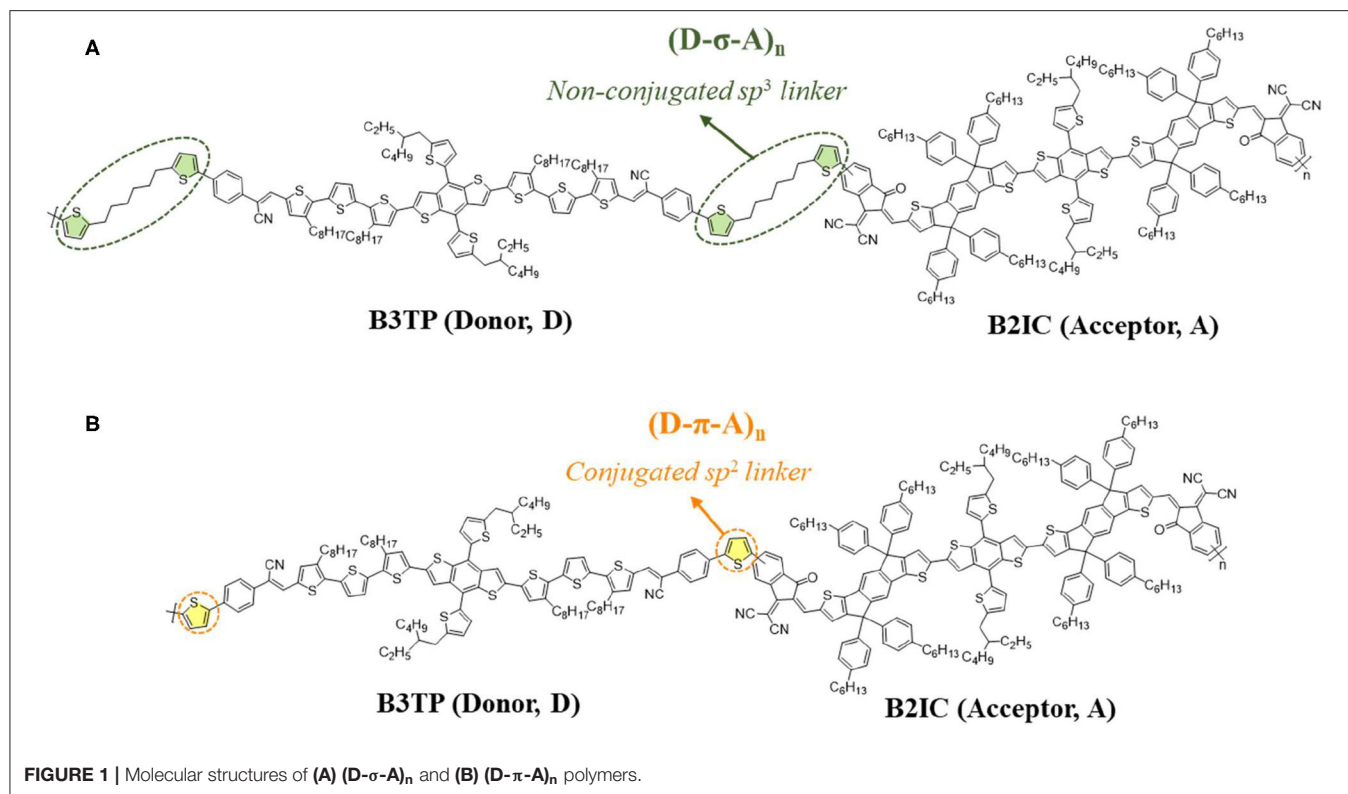
Compound (**D- σ -A**)_n

In a Schlenk tube, **M1** (85.3 mg, 28.8 μ mol), **M2** (75 mg, 28.8 μ mol), Pd₂(dba)₃ (1.3 mg, 5 mol%), and P(*o*-tolyl)₃ (1.75 mg, 10 mol%) were dissolved in toluene (4 mL). The degassed binary mixture was stirred at 180°C for 2 h and subjected to cross-coupling Stille reaction under optimized microwave irradiation. The synthesized crude polymers were purified by precipitation into methanol, followed by Soxhlet extraction to remove unreacted monomers, undesired byproducts, and low-molecular-weight materials, using acetone, hexane, and dichloromethane in succession. The polymer solution was precipitated from methanol, and the solid was filtered to obtain polymer (**D- σ -A**)_n as a black solid [M_n = 24.04 kDa, polydispersity index (PDI) = 2.4]. Elemental Anal. Calcd. for (C₃₂₄H₃₅₂N₆O₂S₂₂)_n: C: 76.82; H: 6.96; N: 1.66; S: 13.92. Found: C: 76.18; H: 6.83; N: 1.71; S: 13.62.

Compound (**D- π -A**)_n

In a Schlenk tube, **M1** (130 mg, 44.1 mmol), **M3** (100 mg, 44.1 mmol), and Pd(PPh₃)₄ (5.0 mg, 10 mol%) were dissolved in toluene (4 mL). The synthesis method and reaction conditions were the same as described for the microwave synthesis of (**D- σ -A**)_n. (**D- π -A**)_n is a black solid (M_n = 10.92 kDa, PDI = 2.3). Elemental Anal. Calcd. for (C₃₀₄H₃₂₄N₆O₂S₂₀)_n: C: 76.14; H: 6.86; N: 1.78; S: 9.55. Found: C: 75.87; H: 6.76; N: 1.83; S: 9.32.

The chemical structures of (**D- σ -A**)_n and (**D- π -A**)_n were verified by gel permeation chromatography, ¹H nuclear magnetic resonance (NMR; **Supplementary Figures 2, 3**), and elemental analyses (EA). The M_n values of the intermediate (**D- σ -A**)_n block and the final (**D- π -A**)_n were 20.0 and 10.9 kg mol⁻¹, respectively, and the corresponding PDI values were 2.4 and 2.3, respectively. Because the molecular weight of the repeating units consisting of the large monomers is over 5,000 g/mol, the molar ratio of the (**D- σ -A**)_n and (**D- π -A**)_n repeating units was determined to be 1:1 from NMR spectra and theoretical EA calculations.



RESULTS AND DISCUSSION

Design, Synthesis, and Characterization

The acceptor-donor-acceptor (A-D-A) backbone architecture of donor and acceptor monomers has drawn particular interest because of the easily tuned energy levels of these species. The benzo[1,2-*b*:4,5-*b'*]dithiophene (BDT) unit used as the main core of π -extended donor and acceptor monomers in this study has become one of the most widely used polymer backbones because of its rigid planar conjugated structure, which can enhance electron delocalization and promote cofacial π - π stacking interactions in the solid state (Wang et al., 2018).

A design strategy for preparing effective A-D-A type donor monomers with narrow bandgaps involves increasing the electron donating ability of the donor monomers by extending the effective π conjugation length. The extended π -conjugated structure with three thiophenes increases the stiffness of the donor backbone. **B3TP**, as an A-D-A type conjugated donor monomer, was designed as shown in **Figure 1**. In **B3TP**, alkyl-substituted terthiophene moieties are added at both ends of the BDT core (Yang et al., 2018) and electron-withdrawing phenylacetonitrile groups are attached as the end-capped group, which guarantees a symmetric and planar structure. As an effective π -extended acceptor monomer, **B2IC** was designed in an acceptor-donor1-donor2-donor1-acceptor (A-D1-D2-D1-A) structure, as shown in **Figure 1**. Such A-D1-D2-D1-A type acceptors have rarely been reported. **B2IC** consists of the BDT core (D2) with indaceno[2,1-*b*:6,5-*b'*]dithiophene

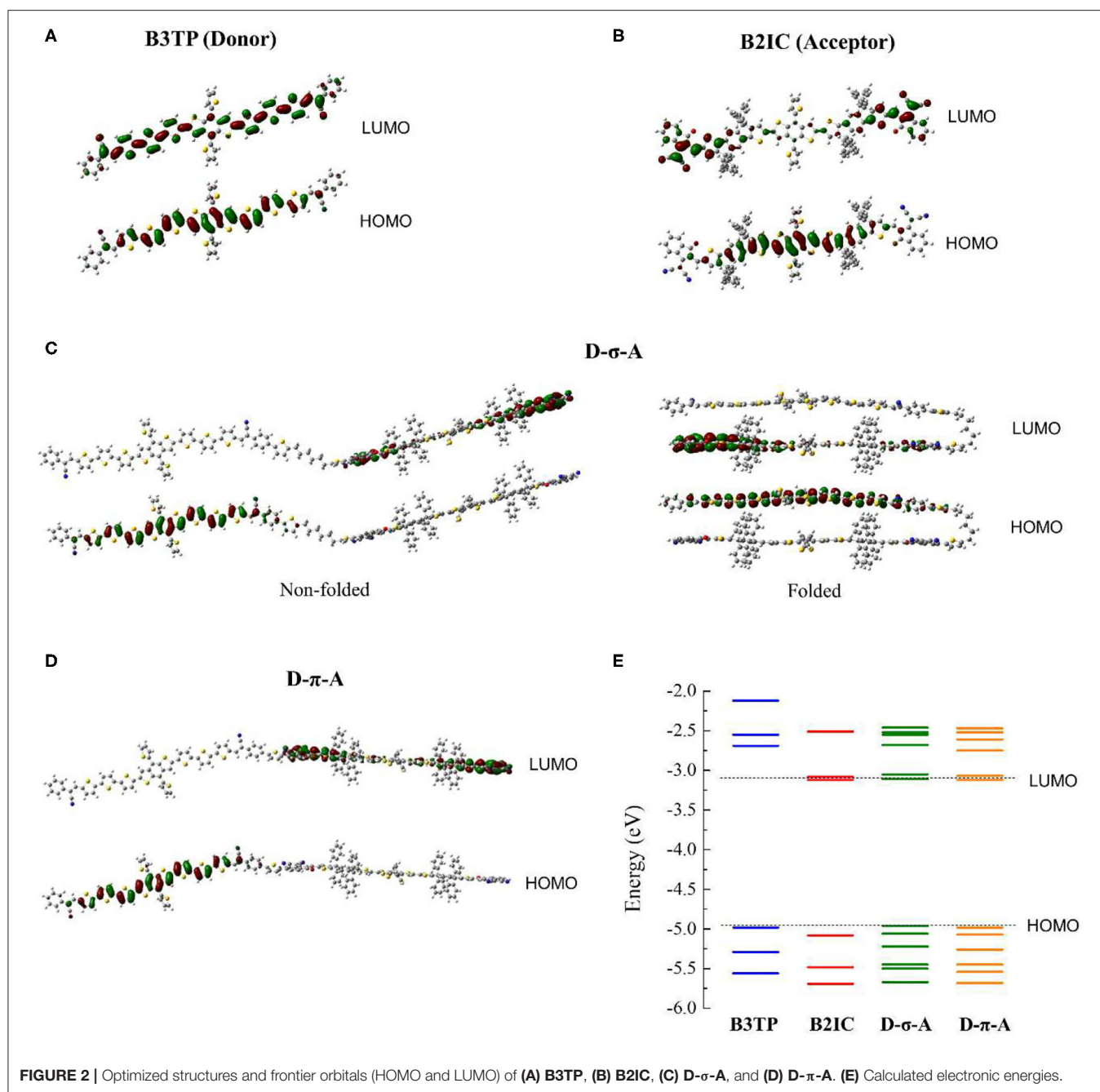
moieties as an additional donor unit (D1) and the end-capping groups of 1,1-dicyanomethylene-3-indanone (IC) as an accepting unit (A).

In dyad systems, photoinduced energy transfer or photoinduced electron transfer is interesting photophysical phenomena that significantly depend on the linker type and length. To study such phenomena, we synthesized $(D-\sigma-A)_n$ and $(D-\pi-A)_n$ polymers by connecting the donor (**B3TP**) and acceptor (**B2IC**) units using an sp^2 type conjugated linker (thiophene) and sp^3 type non-conjugated linker. A detailed investigation of the photophysical properties is presented in the following sections.

Theoretical Studies of π -Extended Monomers, $(D-\sigma-A)$ and $(D-\pi-A)$

To study the electronic and optical properties, density functional theory (DFT) calculations [B3LYP/6-31g(d) and B3LYP-d3/6-31g(d)] were carried out. First, the optimized structures of **B3TP**, **B2IC**, $D-\sigma-A$, and $D-\pi-A$ were obtained. The frontier orbitals (HOMO and LUMO) and natural transition orbitals (NTOs) were calculated. **Figures 2A,B** show the optimized structures and the HOMO and LUMO of **B3TP** and **B2IC**, respectively. The donor monomer, **B3TP** (A-D-A type), and the acceptor monomer, **B2IC** (A-D1-D2-D1-A type), are both planar and fully conjugated. Both **B3TP** and **B2IC** exhibit intramolecular charge transfer upon electronic transition (**Supplementary Figure 4**).

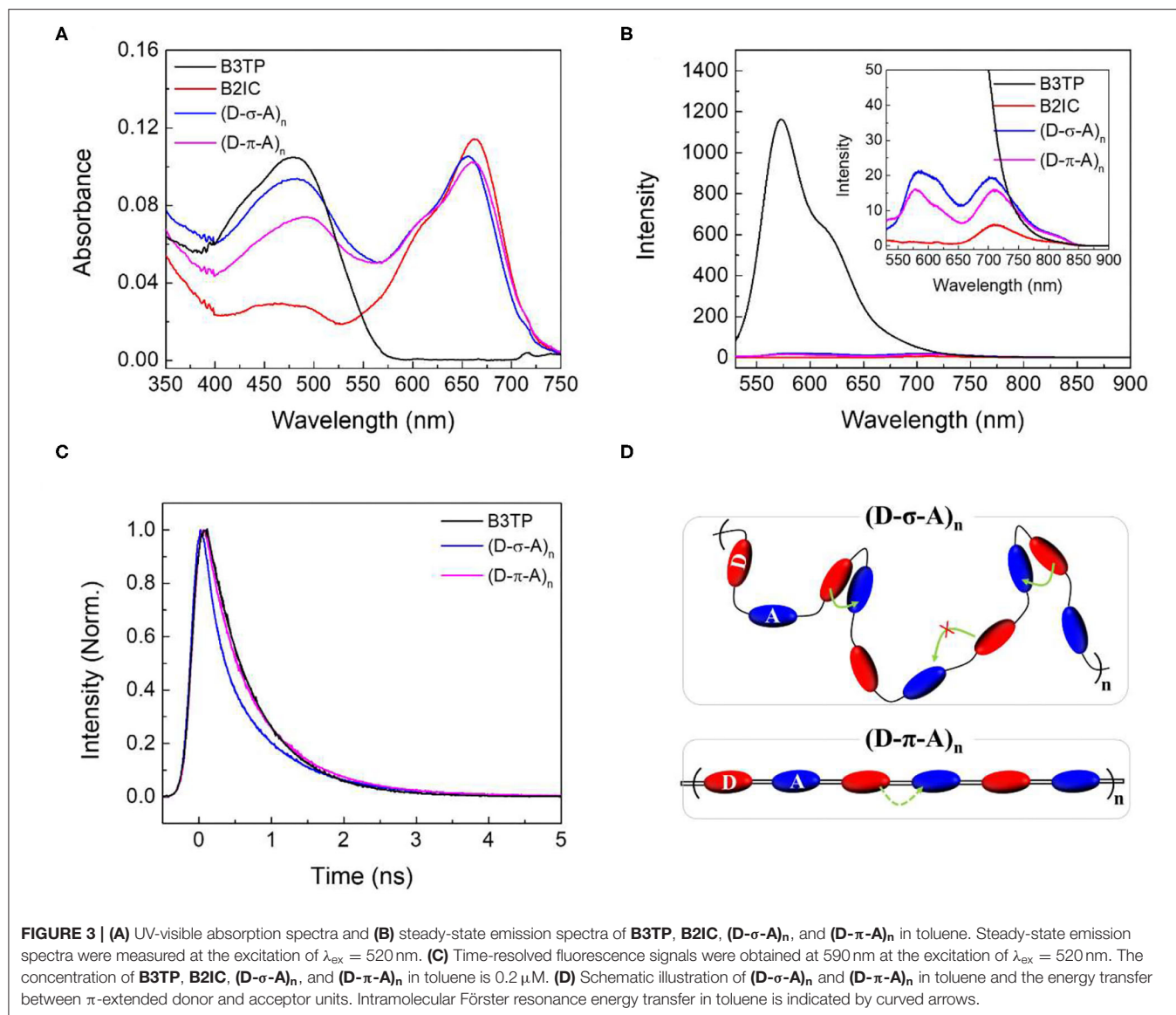
The optimized structures and frontier orbitals of $D-\sigma-A$ and $D-\pi-A$ are shown in **Figure 2**. Note that the folded



structure of D-σ-A in Figure 2 is also energetically stable and can possibly be populated. Because D-σ-A and D-π-A have the same donor and acceptor units, but different linkers (sp^3 vs. sp^2) between the donor and acceptor units, the calculated electronic energies of the HOMO and LUMO levels are almost the same (Figure 2E). For both D-σ-A and D-π-A, the HOMO and LUMO are spatially localized at the π -extended donor and acceptor units, respectively, and exhibit strong charge transfer characteristics, which is directly associated with the photophysical properties of (D-σ-A)_n and (D-π-A)_n, as discussed hereinafter.

Spectroscopic Studies of π -Extended Monomers, (D-σ-A)_n, and (D-π-A)_n

The UV-visible absorption and steady-state emission spectra of B3TP, B2IC, (D-σ-A)_n, and (D-π-A)_n in toluene are shown in Figure 3. The UV-visible absorption spectra of (D-σ-A)_n and (D-π-A)_n are similar, with two absorption peaks near 480 and 660 nm, representing the donor and acceptor units (B3TP and B2IC), respectively. The emission spectrum of B3TP (Figure 3B) exhibits an intense peak at 590 nm ($\lambda_{ex} = 520$ nm), whereas B2IC shows very weak emission at 710 nm. B3TP is nearly planar and structurally rigid, which seems to give a relatively



large fluorescence quantum yield. In contrast, **B2IC** contains 8 phenyl groups in the donor (D1) units, which are flexible and freely rotatable in toluene and might be responsible for significant fluorescence quenching.

As shown in the inset of **Figure 3B**, **(D-σ-A)_n** and **(D-π-A)_n** exhibit two emission peaks at 590 and 710 nm ($\lambda_{ex} = 520$ nm), resulting from **B3TP** and **B2IC**, respectively. However, the overall fluorescence of **(D-σ-A)_n** and **(D-π-A)_n** is significantly quenched when compared with that of **B3TP**. This observation can be readily explained based on the fluorescence properties of **B3TP** and **B2IC** as follows. The donor units (**B3TP**) in **(D-σ-A)_n** and **(D-π-A)_n** are directly excited by 520 nm photons. The excited donor units in **(D-σ-A)_n** and **(D-π-A)_n** undergo Förster resonance energy transfer (FRET) to the acceptor units (**B2IC**) in **(D-σ-A)_n** and **(D-π-A)_n**, owing to which, the fluorescence is quenched. FRET is readily possible in **(D-σ-A)_n** and **(D-π-A)_n** because the emission spectrum of the donor

(**B3TP**) and UV-visible absorption spectrum of the acceptor (**B2IC**) overlap (**Supplementary Figure 5**), and the distance between the donor and acceptor units in the polymer backbones is sufficiently small.

To further understand the fluorescence quenching, the TRF signals of **B3TP**, **(D-σ-A)_n**, and **(D-π-A)_n** in toluene were measured using the time-correlated single-photon counting method, as shown in **Figure 3C**. **B3TP**, **(D-σ-A)_n**, and **(D-π-A)_n** in toluene were excited by 520 nm laser pulses and their TRF signals were measured at 590 nm to monitor the emission of the donor monomers (**B3TP**). The TRF signal of **(D-σ-A)_n** (**Figure 3C**) decayed faster than that of **B3TP** and **(D-π-A)_n** in toluene. The TRF signals were fitted to a multi-exponential function, and the average fluorescence lifetimes are summarized in **Table 1**. The average fluorescence lifetimes ($\tau_{avg} = 0.67$ ns) of **B3TP** and **(D-π-A)_n** in toluene are the same within experimental error, even though the initial TRF decay of **(D-π-A)_n** is slightly

TABLE 1 | Exponential fit of time-resolved fluorescence signals, $S(t) = \sum_i A_i \exp(-t/\tau_i)$, of **B3TP**, **(D- σ -A)_n**, and **(D- π -A)_n** in toluene and films.

	B3TP		(D-σ-A)_n		(D-π-A)_n	
	Toluene	Film	Toluene	Film	Toluene	Film
A_1	0.94	0.77	0.46	0.98	0.30	0.97
τ_1	0.64 ns	0.16 ns	0.17 ns	0.10 ns	0.32 ns	0.11 ns
A_2	0.06	0.23	0.52	0.02	0.69	0.03
τ_2	1.1 ns	0.54 ns	0.79 ns	0.64 ns	0.79 ns	0.70 ns
A_3	–	–	0.02	–	0.01	–
τ_3	–	–	2.4 ns	–	2.8 ns	–
τ_{avg}	0.67 ns	0.25 ns	0.54 ns	0.11 ns	0.67 ns	0.13 ns

The average lifetime was calculated as $\tau_{\text{avg}} = \sum_i A_i \tau_i / \sum_i A_i$.

faster than that of **B3TP**. The average fluorescence lifetime ($\tau_{\text{avg}} = 0.54$ ns) of **(D- σ -A)_n** in toluene is slightly shorter than that of **B3TP** and **(D- π -A)_n**. The difference in the TRF signals of **(D- σ -A)_n** and **(D- π -A)_n** in toluene results from their structural difference, caused by the linkers between the donor and acceptor units, as illustrated in **Figure 3D**. In **(D- π -A)_n**, the π -conjugated linker (sp^2) between the donor and acceptor units is rigid, which fixes the donor and acceptor far from each other, as shown in **Figure 3D**. Therefore, FRET between the donor and acceptor units in **(D- π -A)_n** is less likely. In contrast, in **(D- σ -A)_n**, the sp^3 alkyl chain between the donor and acceptor units is flexible; thus, a folded structure can feasibly be formed as shown in **Figure 2C**. Thus, intramolecular FRET between the donor and acceptor units in the folded sections of **(D- σ -A)_n** is likely, as schematically illustrated in **Figure 3D**. The optical properties of **B3TP**, **B2IC**, **(D- σ -A)_n**, and **(D- π -A)_n** in the films were further studied, as shown in **Figure 4**. The UV-visible absorption spectra of **B3TP**, **B2IC**, **(D- σ -A)_n**, and **(D- π -A)_n** in the films were slightly red-shifted relative to those in toluene (**Supplementary Figure 6**). The spectral features indicate that the donor and acceptor units are closely packed and intermingled in the films, as illustrated in **Figure 5A**. This structural arrangement in the films leads to a significant change in the fluorescence properties of **(D- σ -A)_n** and **(D- π -A)_n**. The steady-state emission spectra of **(D- σ -A)_n** and **(D- π -A)_n** in **Figure 4B** show the emission peak of the acceptor monomers (**B2IC**). This indicates completely efficient FRET from the large donor to acceptor units in **(D- σ -A)_n** and **(D- π -A)_n**. In the films, the donor and acceptor units are closely located so that intermolecular FRET from the donor and acceptor units in **(D- σ -A)_n** and **(D- π -A)_n** becomes very efficient. **Figure 4C** shows the TRF signals of **B3TP**, **(D- σ -A)_n**, and **(D- π -A)_n** in the films. The TRF signal of **B3TP** in the films is found to decay faster than that of **B3TP** in toluene because of the “aggregation causing quenching” effect. The TRF signal of **(D- π -A)_n** in the films decays much faster than that of **(D- π -A)_n** in toluene, resulting from additional intermolecular (or interchain) FRET between the π -extended donor and acceptor units. The TRF signals of the films were fitted by a multi-exponential function, and the average fluorescence lifetimes are summarized in **Table 1**.

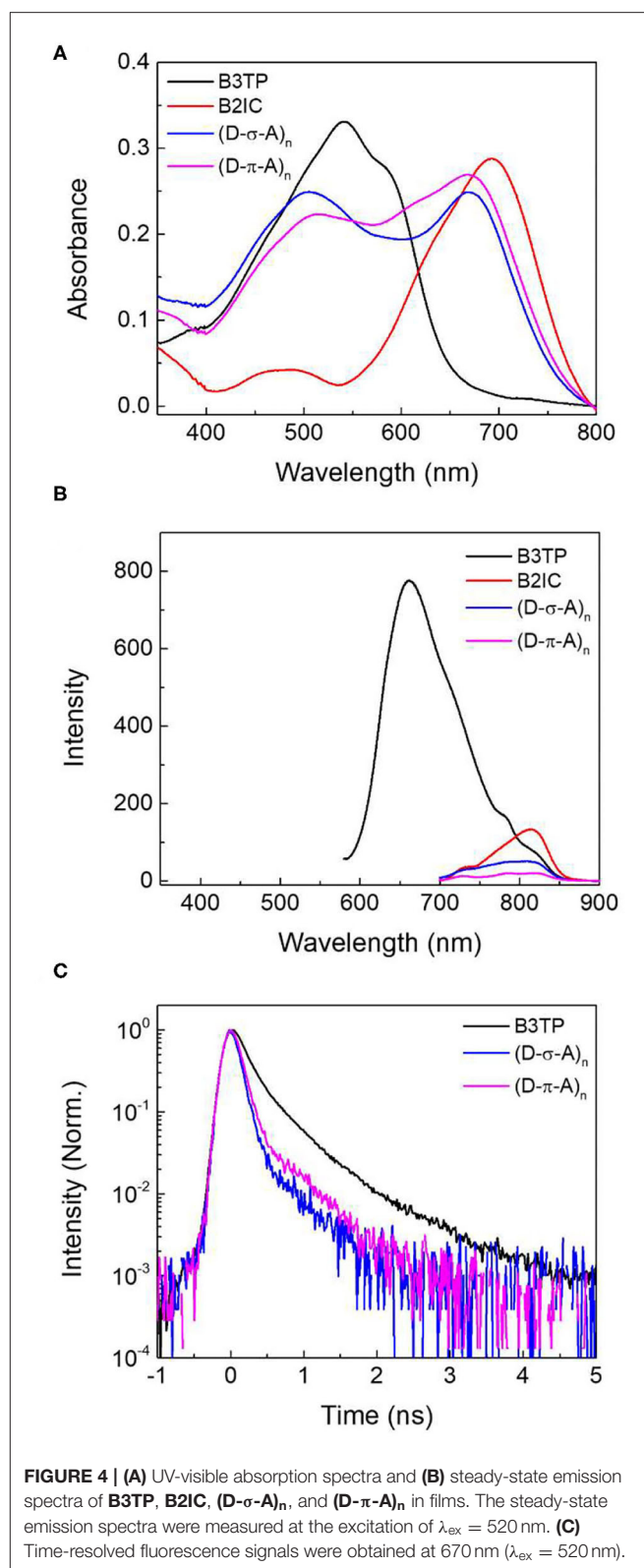
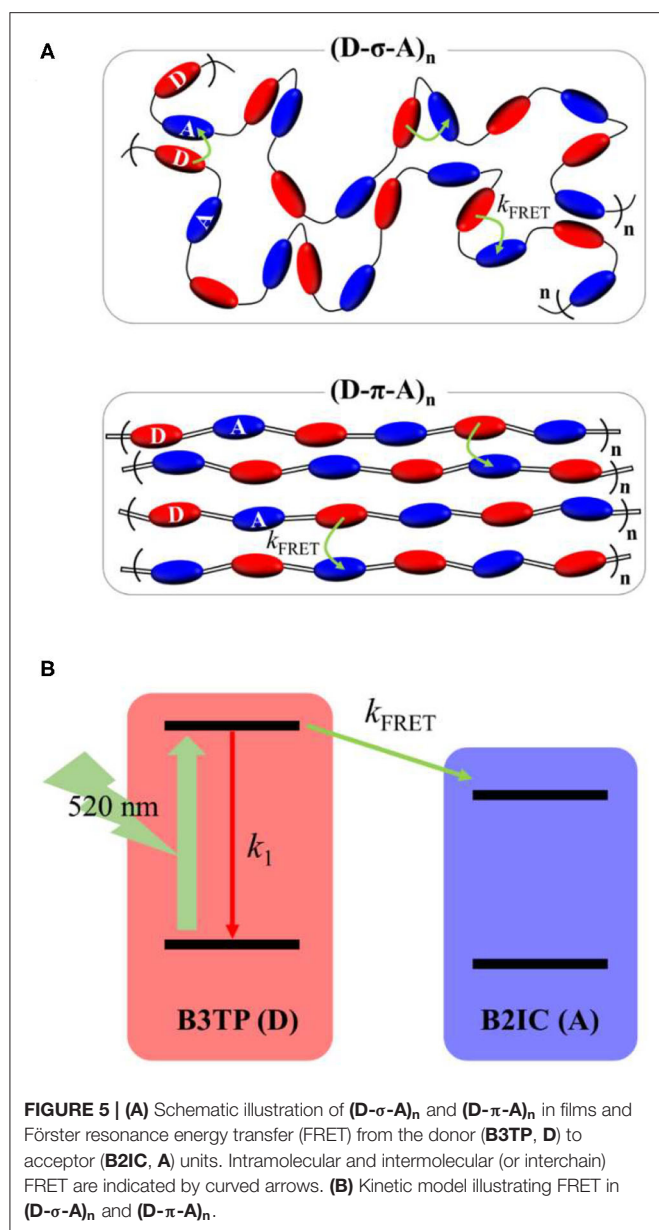


FIGURE 4 | (A) UV-visible absorption spectra and (B) steady-state emission spectra of **B3TP**, **B2IC**, **(D- σ -A)_n**, and **(D- π -A)_n** in films. The steady-state emission spectra were measured at the excitation of $\lambda_{\text{ex}} = 520$ nm. (C) Time-resolved fluorescence signals were obtained at 670 nm ($\lambda_{\text{ex}} = 520$ nm).

By using a simple kinetics model (**Figure 5B**), the intramolecular and intermolecular (or interchain) FRET rate constants can be estimated (**Supplementary Table 1**). As



shown in **Table 1**, the average fluorescence lifetime of **(D-σ-A)_n** ($\tau_{\text{avg}} = 0.54$ ns) in toluene is shorter than that of **B3TP** ($\tau_{\text{avg}} = 0.67$ ns) in toluene because of the intramolecular FRET from the donor units (**B3TP**, **D**) to the acceptor units (**B2IC**, **A**). The intramolecular FRET rate constant of **(D-σ-A)_n** in toluene was estimated to be $k_{\text{FRET}} = 0.36$ ns⁻¹. In the same way, the FRET rate constants of **(D-σ-A)_n** and **(D-π-A)_n** in the films were determined to be $k_{\text{FRET}} = 5.09$ and 3.69 ns⁻¹, respectively. The FRET rate constant was found to be much greater in the films than in toluene. This is because the donor and acceptor units in **(D-σ-A)_n** and **(D-π-A)_n** are much more closely located in the films, and intramolecular and intermolecular FRET are both very efficient in the films, as illustrated in **Figure 5A**.

CONCLUSIONS

To study the role of linkers in energy transfer, we designed and synthesized two dyad polymer systems. First, the π -extended donor monomers (**B3TP**, **D**) with an A-D-A structure and the π -extended acceptor monomers (**B2IC**, **A**) with an A-D1-D2-D1-A structure were synthesized. These donor and acceptor units were linked together by two different linkers (non-conjugated alkyl and π -conjugated linker) to synthesize two types of D-A repeating polymers, **(D-σ-A)_n** and **(D-π-A)_n**.

The photophysical properties of **(D-σ-A)_n** and **(D-π-A)_n** were comprehensively investigated by UV-visible absorption, steady-state emission, and TRF spectroscopy, in conjunction with DFT calculations. DFT calculations show that the π -extended donor and acceptor monomers (**B3TP** and **B2IC**) are planar; **D-σ-A** and **D-π-A** have similar energy profiles, originating from the donor and acceptor units, and exhibit intramolecular charge transfer characteristics upon electronic excitation. A folded structure is possible for **(D-σ-A)_n** because of the flexible non-conjugated alkyl linkers. **(D-σ-A)_n** and **(D-π-A)_n** exhibit similar UV-visible absorption properties. Their fluorescence was found to be quenched due to FRET from the large donor to acceptor units in **(D-σ-A)_n** and **(D-π-A)_n**. In toluene, FRET is more efficient for **(D-σ-A)_n** than for **(D-π-A)_n**. It is likely that the donor and acceptor units are more closely located in the folded structure of **(D-σ-A)_n**, which increases the speed of FRET. In the films, the fluorescence of **(D-σ-A)_n** is more significantly quenched than that of **(D-π-A)_n**, and intramolecular and intermolecular (or interchain) FRET occur more efficiently. The FRET rate constants were determined using a simple kinetics model.

For the two conjugated polymers bearing π -extended donor and acceptor monomers, the linkers between the donor and acceptor units are shown to play an important role in determining the overall structure of the polymers, thereby influencing the optical properties. The flexible alkyl linkers in the repeating group of the polymers lead to more structural freedom in solution, while the rigid π -conjugated linkers provide less flexibility to the fully conjugated polymers. This structural flexibility can significantly impact the optical properties, and can be tailored depending on the application of the donor- and acceptor-based conjugated polymers for a wide range of research fields.

DATA AVAILABILITY STATEMENT

The original contributions presented in the study are included in the article/**Supplementary Materials**, further inquiries can be directed to the corresponding author/s.

AUTHOR CONTRIBUTIONS

DC and SP conceived the research. Chemical synthesis was carried out by NK, SHP, and MC. Spectroscopic experiments and DFT calculations were done by YK. YK and SP analyzed

the spectroscopic data. NK, YK, DC, and SP wrote the manuscript. All authors contributed to the article and approved the submitted version.

FUNDING

This work was supported by the National Research Foundation of Korea (NRF-2020R11A1A01066897, 2019R1A2C2002647, and 2019R1A6A1A11044070) and Korea University-Future Research Grant (KU-FRG).

REFERENCES

- Badgurjar, D., Sudhakar, K., Jain, K., Kalantri, V., Venkatesh, Y., Duvva, N., et al. (2016). Ultrafast intramolecular photoinduced energy transfer events in benzothiazole-borondipyrromethene donor-acceptor dyads. *J. Phys. Chem. C* 120, 16305–16321. doi: 10.1021/acs.jpcc.6b03668
- Caprasecca, S., and Mennucci, B. (2014). Excitation energy transfer in donor-bridge-acceptor systems: a combined quantum-mechanical/classical analysis of the role of the bridge and the solvent. *J. Phys. Chem. A* 118, 6484–6491. doi: 10.1021/jp502815r
- Duvel, G., Grilj, J., and Vauthey, E. (2013). Ultrafast long-distance excitation energy transport in donor-bridge-acceptor systems. *J. Phys. Chem. A* 117, 918–928. doi: 10.1021/jp311540x
- Feng, G., Li, J., He, Y., Zheng, W., Wang, J., Li, C., et al. (2019). Thermal-driven phase separation of double-cable polymers enables efficient single-component organic solar cells. *Joule* 3, 1765–1781. doi: 10.1016/j.joule.2019.05.008
- Jones, G. A., and Bradshaw, D. S. (2019). Resonance energy transfer: from fundamental theory to recent applications. *Front. Phys.* 7:100. doi: 10.3389/fphy.2019.00100
- Jose, J., Ueno, Y., Castro, J. C., Li, L., and Burgess, K. (2009). Energy transfer dyads based on Nile Red. *Tetrahed. Lett.* 50, 6442–6445. doi: 10.1016/j.tetlet.2009.08.130
- Kuss-Petermann, M., Wolf, H., Stalke, D., and Wenger, O. S. (2012). Influence of donor-acceptor distance variation on photoinduced electron and proton transfer in rhenium(I)-phenol dyads. *J. Am. Chem. Soc.* 134, 12844–12854. doi: 10.1021/ja3053046
- Lee, D. H., Lee, J. H., Kim, H. J., Choi, S., Park, G. E., Cho, M. J., et al. (2017). (D)n- σ -(A)m type partially conjugated block copolymer and its performance in single-component polymer solar cells. *J. Mater. Chem. A* 5, 9745–9751. doi: 10.1039/C7TA01819C
- Li, C., Wu, X., Sui, X., Wu, H., Wang, C., Feng, G., et al. (2019). Crystalline cooperativity of donor and acceptor segments in double-cable conjugated polymers toward efficient single-component organic solar cells. *Angew. Chem. Int. Ed. Engl.* 58, 15532–15540. doi: 10.1002/anie.201910489
- Murphy, C. B., Zhang, Y., Troxler, T., Ferry, V., Martin, J. J., and Jones, W. E. (2004). Probing Förster and Dexter energy-transfer mechanisms in fluorescent conjugated polymer chemosensors. *J. Phys. Chem. B* 108, 1537–1543. doi: 10.1021/jp0301406

ACKNOWLEDGMENTS

MALDI-TOF mass spectra were obtained at the Korea Basic Science Institute (Seoul Center).

SUPPLEMENTARY MATERIAL

The Supplementary Material for this article can be found online at: <https://www.frontiersin.org/articles/10.3389/fchem.2020.605403/full#supplementary-material>

- Scholes, G. D. (2003). Long-range resonance energy transfer in molecular systems. *Annu. Rev. Phys. Chem.* 54, 57–87. doi: 10.1146/annurev.physchem.54.011002.103746
- Schwartz, B. J. (2003). Conjugated polymers as molecular materials: how chain conformation and film morphology influence energy transfer and interchain interactions. *Annu. Rev. Phys. Chem.* 54, 141–172. doi: 10.1146/annurev.physchem.54.011002.103811
- Villamaina, D., Bhosale, S. V., Langford, S. J., and Vauthey, E. (2013). Excited-state dynamics of porphyrin-naphthalenedimide-porphyrin triads. *Phys. Chem. Chem. Phys.* 15, 1177–1187. doi: 10.1039/C2CP43595K
- Wang, L., Pan, C., Chen, Z., Zhou, X., Gao, C., and Wang, L. (2018). A study of the thermoelectric properties of benzo[1,2-b:4,5-b']dithiophene-based donor-acceptor conjugated polymers. *Polym. Chem.* 9, 4440–4447. doi: 10.1039/C8PY00812D
- Wang, S., Bohnsack, M., Megow, S., Renth, F., and Temps, F. (2019). Ultrafast excitation energy transfer in a benzimidazole-naphthopyran donor-acceptor dyad. *Phys. Chem. Chem. Phys.* 21, 2080–2092. doi: 10.1039/C8CP05054F
- Wiebeler, C., Plasser, F., Hedley, G. J., Ruseckas, A., Samuel, I. D., and Schumacher, S. (2017). Ultrafast electronic energy transfer in an orthogonal molecular dyad. *J. Phys. Chem. Lett.* 8, 1086–1092. doi: 10.1021/acs.jpcllett.7b00089
- Wu, P., and Brand, L. (1994). Resonance energy transfer: methods and applications. *Anal. Biochem.* 218, 1–13. doi: 10.1006/abio.1994.1134
- Yang, Y., Wang, K., Li, G., Ran, X., Song, X., Gasparini, N., et al. (2018). Fluorination triggered new small molecule donor materials for efficient as-cast organic solar cells. *Small* 14:e1801542. doi: 10.1002/sml.201801542

Conflict of Interest: The authors declare that the research was conducted in the absence of any commercial or financial relationships that could be construed as a potential conflict of interest.

Copyright © 2020 Kim, Kwon, Park, Cho, Choi and Park. This is an open-access article distributed under the terms of the Creative Commons Attribution License (CC BY). The use, distribution or reproduction in other forums is permitted, provided the original author(s) and the copyright owner(s) are credited and that the original publication in this journal is cited, in accordance with accepted academic practice. No use, distribution or reproduction is permitted which does not comply with these terms.